AJNR Am J Neuroradiol 19:1235–1240, August 1998

MR-Guided Endoscopic Sinus Surgery

Liangge Hsu, Marvin P. Fried, and Ferenc A. Jolesz

Summary: We describe an interactive, intraoperative imaging-guided method for performing endoscopic sinus surgery (ESS) within a vertically open MR system. The procedure was performed with intraoperative imaging using a 0.5-T magnet with a 56-cm vertical gap. Interactive control of imaging planes was accomplished by optical tracking with two infrared light-emitting diodes mounted on an aspirator probe. The probe's position defined the location of the orthogonal imaging planes. Twelve patients with varying degrees of sinus disease underwent ESS with MR imaging guidance. Patients had acute and chronic sinusitis, nasal polyposis causing airway obstruction, or tumor requiring tissue biopsy. All procedures were performed with the patients under general anesthesia. The integration of endoscopy with optical tracking and intraoperative interactive imaging allowed localization of anatomic landmarks during ESS. No complications were encountered.

Endoscopic sinus surgery (ESS) is an effective, minimally invasive procedure used to correct disease of the ostiomeatal complex and paranasal sinuses (1, 2). Sinus disease is often due to obstruction at the ostiomeatal complex (3). Correction of the obstruction may lead to reversible recovery of the diseased sinus mucosa. Minimally invasive surgery produces less tissue injury and promotes faster healing. Serious complications, however, may occur because of the proximity of the paranasal sinuses to vital surrounding structures, such as the orbit, anterior cranial fossa, pituitary fossa, internal carotid arteries, and cavernous sinus. The most serious complications are blindness, intracranial hemorrhage, and CSF leakage (4, 5). Endoscopy provides a view of the surface anatomy but without the benefit of depth perception. Visualization and orientation is particularly problematic when the surgeon encounters bleeding within the operative field or when normal anatomy has been distorted by previous surgery.

In the past, intraoperative guidance has been effected by fluoroscopy (6). Recently, preoperative CT-based navigational systems have become available (7–10). This imaging-guided system entails preoperative acquisition of axial cross-sectional images and reconstruction of orthogonal planes that are displayed intraoperatively. Registration to the patient's anatomy is necessary before ESS begins, and these navigational systems do not provide updated intraoperative information if the anatomy is altered during surgery. The main advantage of the near real-time MR-guided system lies in its ability to update current information about the anatomy as the procedure is performed. MR imaging, with its ability to provide excellent soft-tissue differentiation and information about surrounding vasculature noninvasively, can also facilitate the monitoring of disease removal; moreover, no ionizing radiation is involved in this system.

Methods

Technique

We used a 0.5-T open-configuration magnet (Signa SP, General Electric Medical Systems, Milwaukee, WI) with a vertical gap that provided direct access to the patient (11, 12). The surgeon and an assistant usually stood across from each other within the 56-cm gap. In the operating room of the MR interventional suite, all anesthesia (XL10 MRI Compatible Anesthesia Station; Ohmeda, Madison, WI) and monitoring equipment systems (MagLife ODAM; Bruker, Wissembourg,

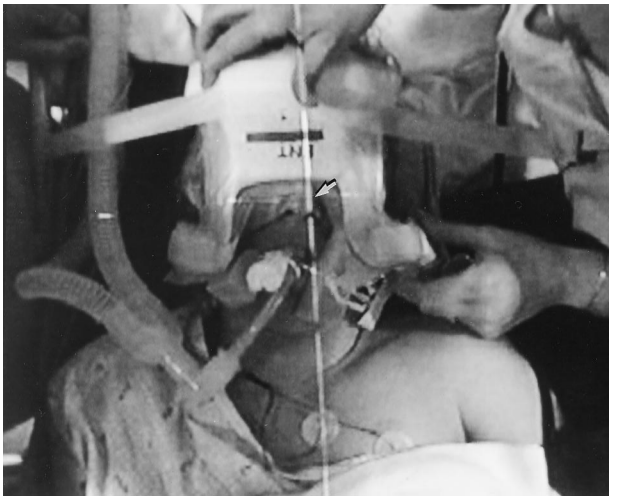

FIG 1. Overhead view of placement of flexible transmit-and-receive coil around the sinuses with the patient intubated. The horizontal and vertical light bars allow optimum positioning of coil in the center of the homogeneous field, shown here as the intersection of the light bars (*arrow*).

Received January 16, 1997; accepted after revision November 21.

From the Departments of Radiology (L.H., F.A.J.) and Otology & Laryngology (M.P.F.), Harvard Medical School, Brigham and Women's Hospital, Boston, MA.

Address reprint requests to Liangge Hsu, MD, Brigham and Women's Hospital, 75 Francis St, Boston, MA 02115.

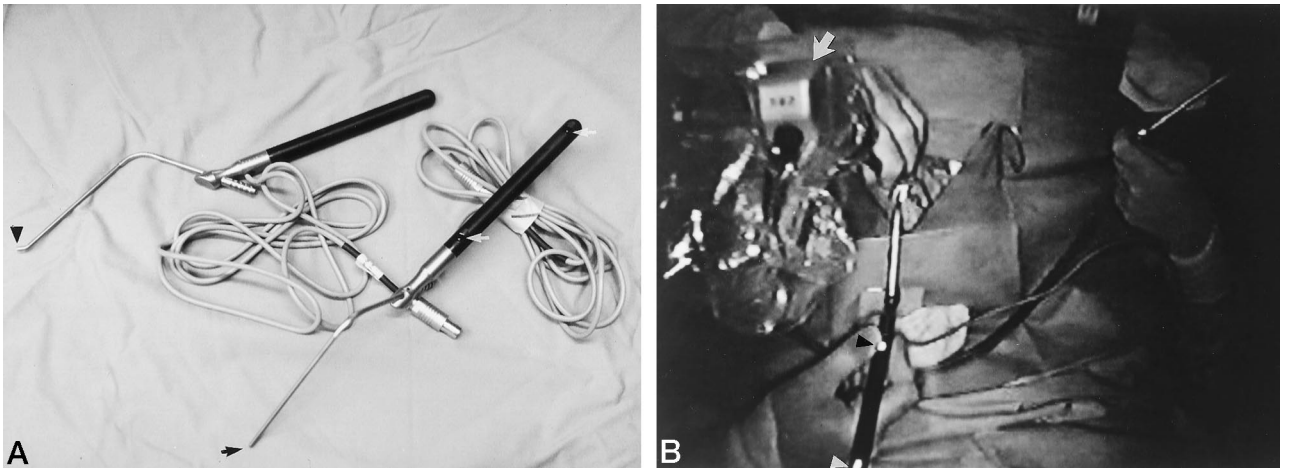

FIG 2. *A*, Two LEDs (*white arrows*) mounted on two aspirator probes with both a straight (*black arrow*) and an angled (*arrowhead*) tip.
B, Overhead view of near real-time localization with LED-mounted aspirator probe (*arrowheads*) in one hand and endoscope in the other (*arrow*).

FIG 3. Patient in supine position within vertical gap of the open-configuration magnet with mounted display monitors (*arrows*) above.

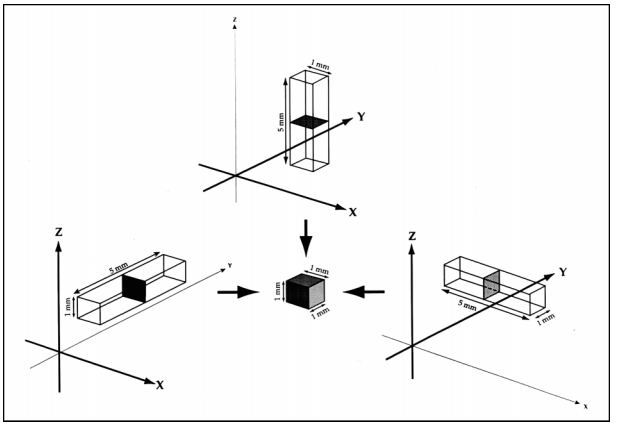

FIG 4. Diagram shows 1-mm spatial resolution of tip position even though section thickness is 5 mm, owing to an approximately 1-mm in-plane resolution for each orthogonal plane.

France) were MR-compatible. Surgical instruments and the endoscope (Storz Surgical Instruments, St Louis, MO) were also MR-compatible and produced no significant artifacts. Communication between the operators and the technologist was established via an audio system.

The transmit-and-receive surface coil was wrapped around the patient's face (Fig 1) and adjusted to allow optimal imaging within a 30-cm-diameter spherical volume from the isocenter of the magnet. Interactive localization was achieved using a 3D optical digitizer system (Integrated Technologies Inc, Boulder, CO) with two infrared light-emitting diodes (LEDs) that were mounted on an aspirator probe (Fig 2). The position of the LEDs was detected by three cameras located above the magnet's isocenter. Spatial information concerning the tip of the aspirator probe generated by the LEDs was fed into a sequential logic box to calculate position and coordinates. Images from three orthogonal planes could then be acquired relative to the position of the tip. These were displayed on a 5-inch liquid crystal display (LCD) monitor mounted within the gap of the magnet (Fig 3). The tip was placed on an intranasal or sinus site and its location appeared on each of three orthogonal MR images as a crosshair annotation. Although the section thickness of each image was 5 mm, the spatial definition of the aspirator tip was about 1 mm, since the image from each plane had about a 1-mm in-plane resolution (Figs 4 and 5). Endoscopic images of the aspirator tip were displayed on a second LCD monitor, thus allowing simultaneous visualization of endoscopic videos and intraoperative MR images (Fig 6).

The initial calibration was achieved by mechanically aligning the sensor system within the isocenter. A software application then correlated the geometric points in the field of view of the pointer system with those in the MR imaging volume. A final verification of the accuracy of the pointer system was made by using a combination pointer device and a 25-cm spherical phantom with 12 registered points at the surface. Image analysis then located the center of the MR image generated at each point and compared them with those reported by the pointer. The average error was 0.55 mm at the isocenter and 0.88 mm at the registered points, with a maximum error of 1.58 mm. The clinical accuracy of the pointer system was also reviewed retrospectively in 27 studies. A comparison between the location of the tip of the actual device and the indicated tip of the scan pointer showed an average distance error of about 1.77 mm.

After the patient was given a general anesthetic and intubated, the surface-flexible coil was placed over the face and above the nose. An initial set of images through the sinuses was displayed in three orthogonal planes just before the start of ESS. During ESS, fast spin-echo T1-weighted images were acquired in orthogonal planes. The position of the two LEDs was tracked by overhead cameras and translated at a workstation into imaging coordinates for the MR imager. The time necessary to acquire images in one plane was determined by the sequence chosen. For multiple-excitation image acquisition, neither the endoscope nor the aspirator probe was necessarily in the field of view. A total of eight excitations can be generated, although we found that four were sufficient (Fig 7).

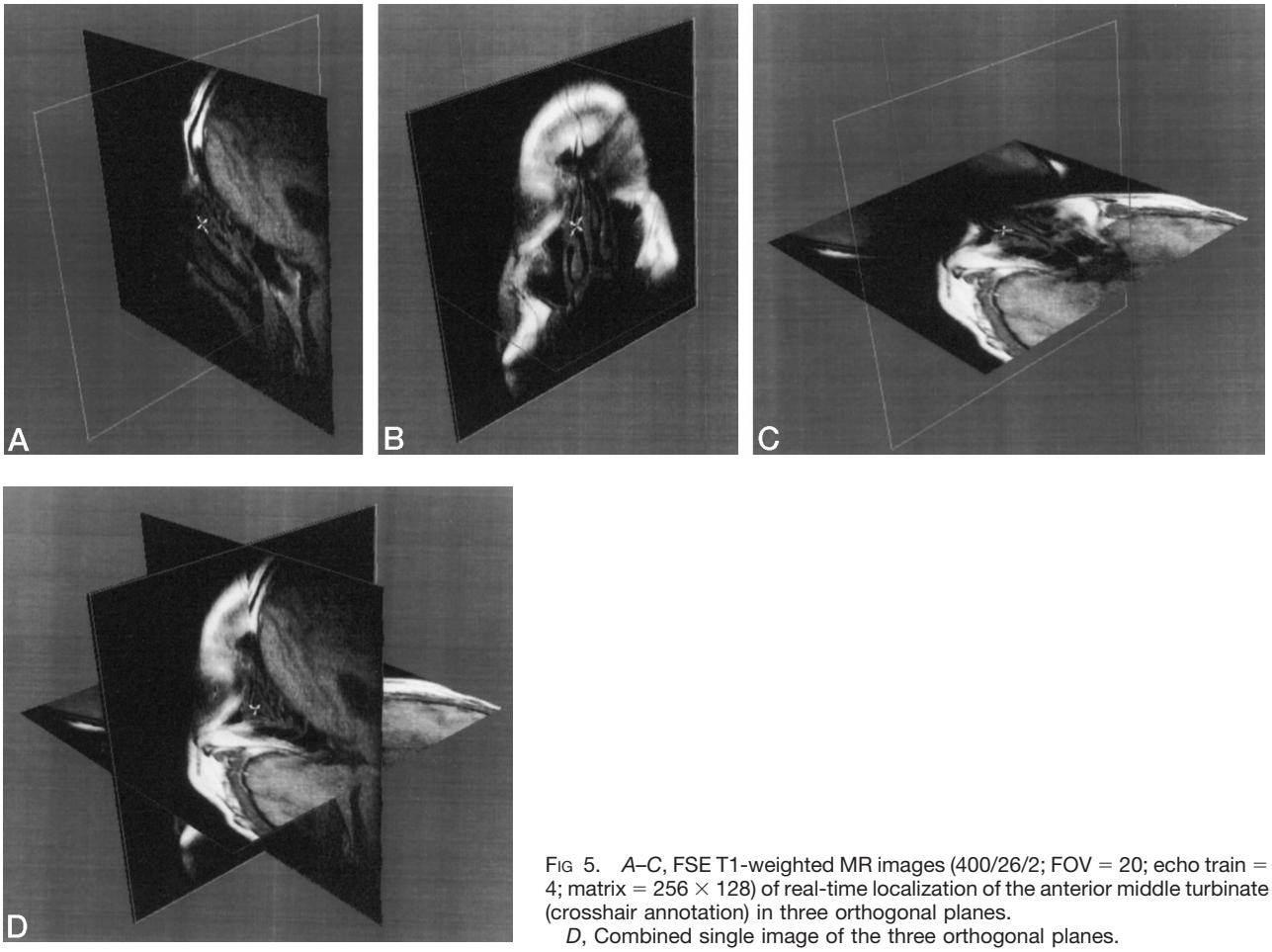

FIG 5. *A–C*, FSE T1-weighted MR images (400/26/2; FOV = 20; echo train = 4; matrix = 256 × 128) of real-time localization of the anterior middle turbinate (crosshair annotation) in three orthogonal planes.
D, Combined single image of the three orthogonal planes.

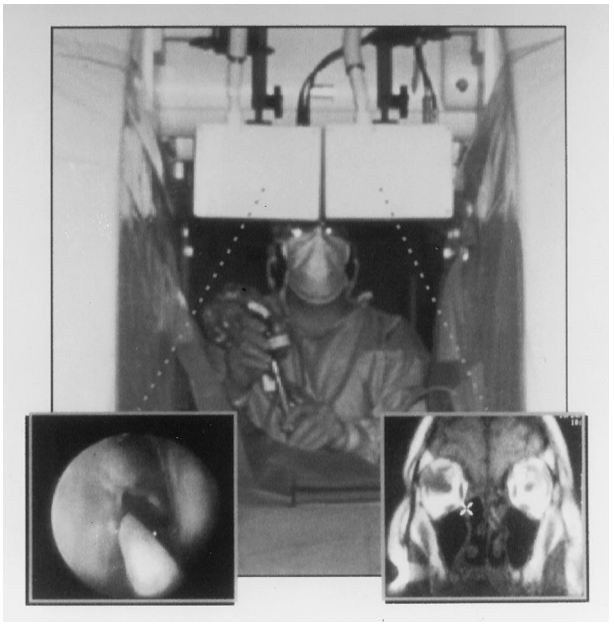

FIG 6. Simultaneous depiction of endoscopic video and real-time MR images of same anatomic site on two LCD monitors.

Initial Patient Experience

Twelve patients (ages 23 to 68 years) underwent ESS in the open magnet after providing informed consent. During ESS, the surgeon interactively viewed the probe in relation to the images, correlating the position of the virtual aspirator tip with that of the actual endoscopic aspirator tip. This correlation was performed visually and communicated by the surgeon at such anatomic sites as the anterior middle turbinate, the lamina papyracea, the maxillary ostium, the frontal ethmoidal recess, and the sphenoidal ostium. These landmarks were chosen because they can be reliably identified on both video endoscopy and on MR images. They were accurately identified at all locations, except in one instance when the instrument was bent. Although the accuracy of placement was not quantified, exactness was established when the tip was positioned at an anatomic landmark identifiable on both endoscopic videos and MR images. Figure 8 illustrates real-time localization of the lamina papyracea and sphenoidal ostium. One patient had a biopsy and resection of a right-sided inflammatory nasal polyp. Another underwent drainage of a right sphenoidal mucocele (Fig 9). No complications were encountered.

Discussion

Numerous studies have reported complications of ESS, ranging from minor, such as synechiae formation (4% to 8%), to more serious, such as orbital and nasolacrimal duct injury (5%), to rare, such as hemorrhage and CSF leak (1%) (4, 13, 14). Without direct intraoperative imaging guidance, the surgeon cannot

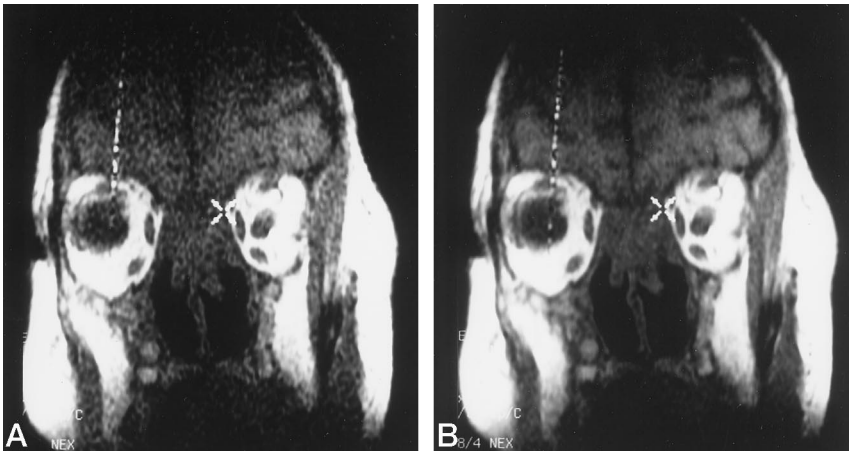

FIG 7. *A* and *B*, Crosshair annotation indicates real-time tip localization of left lamina papyracea at one and four excitations, respectively.

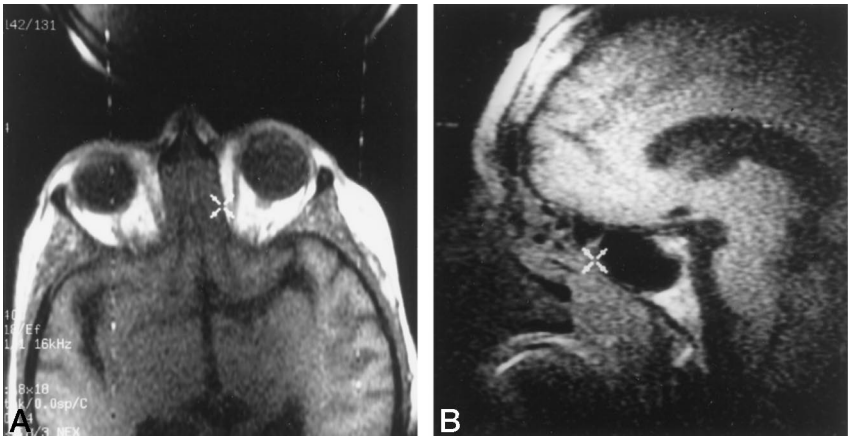

FIG 8. *A* and *B*, FSE T1-weighted 14-second MR images (400/26/2; FOV = 20; echo train = 4; matrix = 256 × 128) show real-time localization (crosshair annotation) of left lamina papyracea and sphenoidal ostium in axial and sagittal planes, respectively.

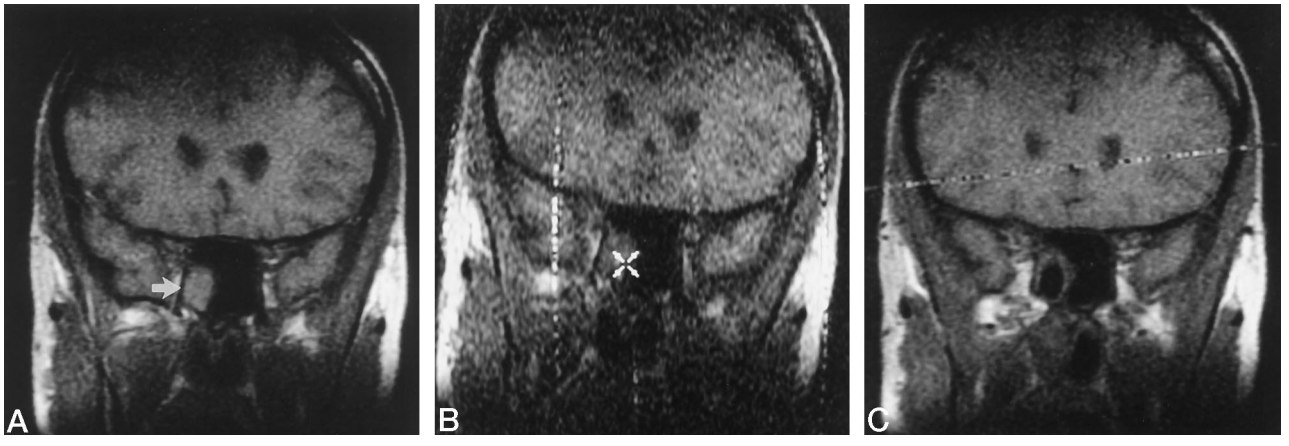

FIG 9. *A–C*, Coronal FSE T1-weighted MR images (400/26/2; FOV = 20; echo train = 4; matrix = 256 × 128) before (*arrow*), during (with crosshair annotation within right sphenoidal sinus), and after drainage of a mucocele in the right sphenoidal sinus.

determine the actual position or movement of surgical instruments relative to surrounding anatomy.

In recent years, there has been an emergence of various navigational devices to interactively display previously acquired CT scans during ESS. The position of the tracking instruments relative to the images is determined by using articulated arms with encoders, optical tracking devices, and electromagnetic sensors (7–10). CT-based navigational systems provide excellent bony detail in a standard operating room environment and do not require special surgical instrumentation. They are thought to improve the ability to navigate through the anatomy and reduce operating time as well as to enhance patient safety. Three-dimensional image representation is provided by image processing and not by the use of intraoperative data. Time is required before ESS to preregister and calibrate the systems to optimize the accuracy of localization.

Intraoperative MR guidance potentially offers several advantages over preoperative CT-based guidance systems. MR imaging provides multiplanar capability

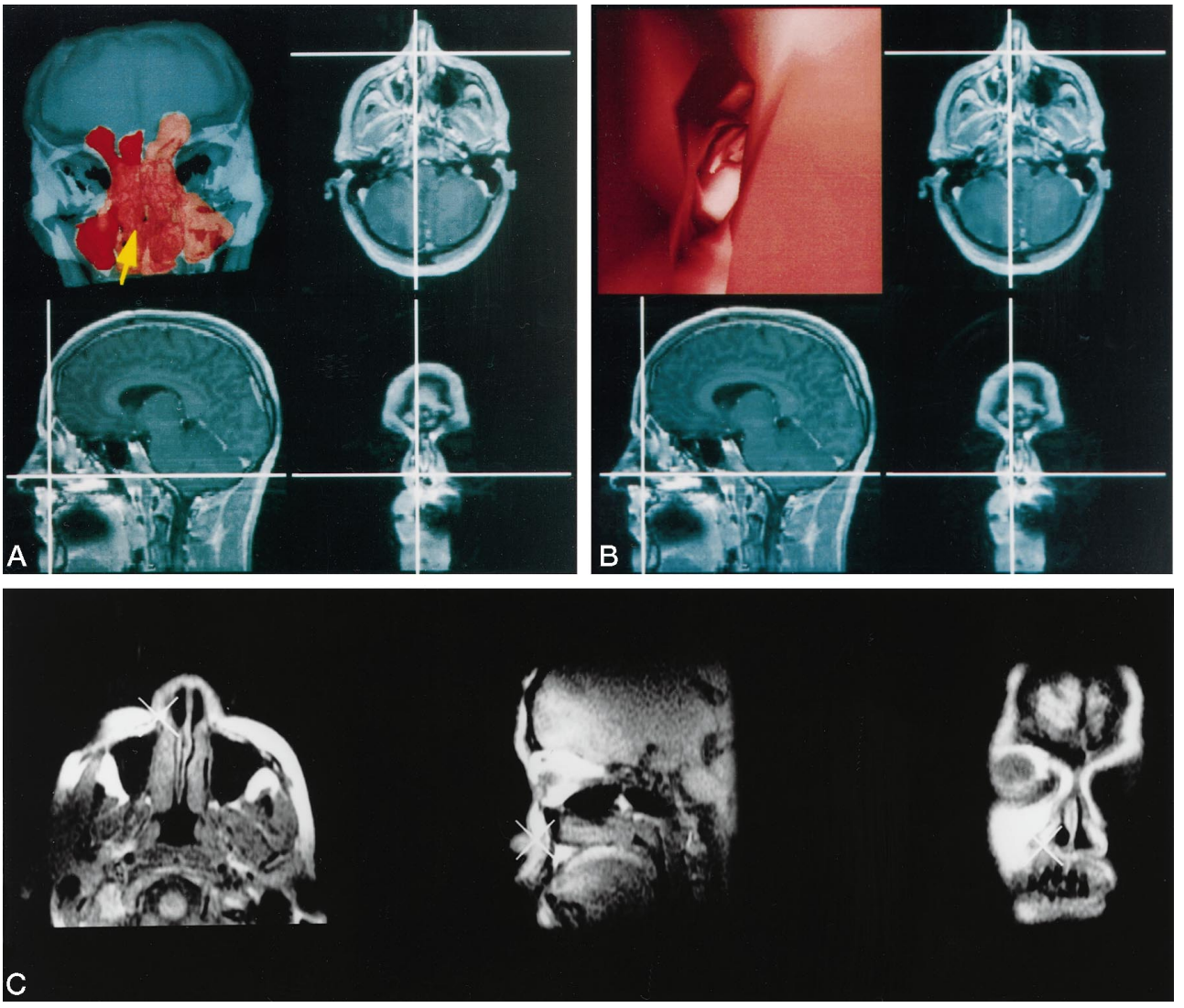

FIG 10. *A*, Three orthogonal spoiled gradient-recalled echo in the steady state 3D MR images (35/5/1; flip angle = 45°; FOV = 24; thickness = 1.5 mm; matrix = 256 × 192) accompanied by 3D coronal reconstruction from MR data (acquired before surgery) (*upper left*) show location of right lateral nasal wall (crosshair and *yellow arrow*).

B, Same MR images as in *A* displayed with virtual endoscopic image generated from preprocedural MR data localizing right lateral nasal wall.

C, Axial, sagittal, and coronal near real-time FSE T1-weighted MR images (400/26/1; FOV = 20; echo train = 4; matrix = 256 × 128) show localization of right lateral nasal wall.

and affords better soft-tissue differentiation than CT. The images are actively acquired during rather than before surgery; thus, if changes in anatomy occur during the procedure, the images are updated to incorporate these changes, enabling more precise intraoperative guidance. Our first clinical experience did not include patients with bony lesions, tumors, or orbital decompression from fractures, as we attempted to limit our initial trial to noncomplex cases. At this early stage of clinical experience, the procedures were also more time-consuming as compared with those performed in a standard operating room, since additional time was necessary for image acquisition. Also, in a limited MR imaging environment and within a smaller working space, a certain degree of adjustment is necessary to achieve optimal results.

An obvious advantage of MR guidance is the soft-tissue detail and depth perception that allows for last-minute adjustments during any part of the procedure. This system was considered particularly helpful in resecting a polyp in a patient whose bilateral disease caused such erosion of the lamina papyracea that the bony landmarks were no longer visible. The type of procedures initially selected do not represent the full potential of this technology. When this method is expanded to skull-base applications, the advantages of intraoperative imaging guidance should become more obvious; for example, the improved visualization during endoscopic surgery may result in substantially reduced procedure times.

To combine the advantages of both CT and MR imaging guidance, we are currently in the process of integrating previously acquired CT scans and/or high-field MR images with intraoperative MR images. The

CT scans will provide detailed delineation of bony anatomy while the high-field, high-resolution MR images will show superior soft-tissue detail. In addition, previously acquired volumetric CT or MR studies can be processed and reconstructed to allow 3D viewing. Virtual endoscopy is a new 3D display technique that uses cross-sectional volumetric imaging. The inner surfaces of organs are reconstructed and the viewer can navigate within the organ. Virtual endoscopy allows the interactive visualization of cavitary organs from the endoscopist's point of view (15). As seen in Figure 10, it is possible to display the position of the tracking probe relative to previously acquired CT or MR images along with intraoperatively acquired open MR images. The intraoperative images can be displayed separately or in combination, and this combined information may help to locate disease and improve the safety of the procedure.

Conclusion

Our initial experience suggests that interactive, intraoperative MR imaging guidance is a safe and feasible alternative to the current preoperatively acquired CT-based navigational systems. This interventional MR imaging system can also be used for biopsies (16) in head and neck procedures in which direct percutaneous or transoral routes are used, especially in cases in which the lesion does not produce mucosal deformity visible at endoscopy. Intraoperative MR guidance of thermal ablation may also be helpful for treating head and neck lesions (17, 18). This technology may also play a role in the development of other diagnostic and therapeutic options, such as staging of aerodigestive tumors by directed biopsy and more accurate radiation seed placement, as well as in the imaging-monitored surgical resection of skull base and neck masses. It may also facilitate the development of new, minimally invasive endoscopic applications that currently are not performed because of the limitations of the endoscope, such as transsphenoidal and other skull base procedures that would benefit from MR imaging guidance.

Acknowledgments

We thank Maureen Ainslie, Angela Roddy Kanan, Holly Ibister, Paul Morrison, and GE Medical systems for their invaluable support and assistance.

References

1. Mafee MF, Chow JM, Meyers R. **Functional endoscopic sinus surgery, anatomy, CT screening, indications and complications.** *AJR Am J Roentgenol* 1993;160:735–744
2. Messerklinger W. **Uber die Drainage der Menschlichen Nasennebenhohler unter normalen und pathologischen Bendingunger. II. Mittlerlung: Die Stirnhohole and ihr Ausfuhrings system.** *Monatsschr Oxrenheilhd* 1967;101:313–326
3. Kennedy DW, Zinreich SJ, Rosenbaum AE, Johns ME. **Functional endoscopic sinus surgery: theory and diagnostic evaluation.** *Arch Otolaryngol* 1985;111:576–582
4. Hudgins PA. **Complications of endoscopic sinus surgery: the role of the radiologist in prevention.** *Radiol Clin North Am* 1993;31:21–32
5. Stankiewicz JA. **Complications of endoscopic intranasal ethmoidectomy.** *Laryngoscope* 1987;97:1270–1273
6. Anon JB. **Intraoperative use of fluoroscopic C-arm during endoscopic intranasal sinus surgery.** *Otolaryngol Head Neck Surg* 1991;2:266
7. Mosges R, Klimek L. **Computer-assisted surgery of the paranasal sinuses.** *J Otolaryngol* 1993;22:69–71
8. Zinreich JS, Tebo SA, Long DM, et al. **Frameless stereotaxic integration of CT imaging data: accuracy and initial applications.** *Radiology* 1993;188:735–742
9. Anon JB, Lipman SP, Oppenheim D, et al. **Computer-assisted endoscopic sinus surgery.** *Laryngoscope* 1994;104:901–905
10. Fried MP, Kleefield J, Taylor R. **A new armless image guidance system for endoscopic sinus surgery.** *Otolaryngol Head Neck Surg* (in press)
11. Schenck JF, Jolesz FA, Roemer PB, et al. **Superconducting open-configuration MR imaging system for image-guided therapy.** *Radiology* 1995;195:805–814
12. Silverman SG, Jolesz FA, Newman RW, et al. **Design and implementation of an interventional MR imaging suite.** *AJR Am J Roentgenol* 1997;168:1465–1471
13. Lane FS, Brindley PC. **Indications, evaluation, complications and results of functional endoscopic sinus surgery in 200 patients.** *Otolaryngol Head Neck Surg* 1993;108:688–696
14. Maniglia AJ. **Fatal and other major complications of endoscopic sinus surgery.** *Laryngoscope* 1991;101:349–354
15. Jolesz FA, Lorenson WE, Shinmoto H, et al. **Interactive virtual endoscopy.** *AJR Am J Roentgenol* 1997;169:1229–1235
16. Silverman SG, Collick BD, Figueira MR, et al. **Interactive MR-guided biopsy in an open-configuration MR imaging system.** *Radiology* 1995;197:175–181
17. Castro DJ, Lufkin RB, Saxton RE, et al. **Metastatic head and neck malignancy treated using MRI guided interstitial laser phototherapy: an initial case report.** *Laryngoscope* 1992;102:26–32
18. Vogl T, Mack M, Muller P, Phillip C. **Recurrent nasopharyngeal tumors: preliminary clinical results with interventional MR imaging-controlled laser induced thermotherapy.** *Radiology* 1995;196:725–733